ISSN: 1231-4005
e-ISSN: 2354-0133
ICID: 1133864
DOI: 10.5604/12314005.1133864

SPATIAL MODEL OF THE UNSPRUNG WHEELED MACHINE'S DYNAMIC SYSTEM

Stefan Chwastek

Krakow University of Technology, Institute of Machine Design
Jana Pawła II Av. 37, 31-864 Krakow, Poland
tel.: +48 12 3743360, fax: +48 12 3743409
e-mail: chwastek@mech.pk.edu.pl

Abstract

Mobile heavy machines as unsprung vehicles exhibit low dissipation ability, hence the ride even at low speeds may give rise to intensive vertical and angular vibration. Vibrations thus produced are mostly in the low-frequency range and hence energy dissipation in tires will reduce the vibration intensity in a minor degree only. Particularly dangerous situations occur when the road wheels break away from the road surface due to the 'galloping' effect. Kinematic excitation acting on the wheels is mostly uncorrelated stochastic (random) processes, giving rise to the "snake meandering" effect. That implies a major restriction on the ride velocity, which negatively affects the machine performance. The motion of tired wheels will always involve certain slipping. While investigating the feasibility of increasing the efficiency of the vibration reduction systems, one ought to take into account the variable adhesion of road wheels due to different dynamic loading acting on the vehicle axles during the ride. This study investigates the motion of unsprung mobile machines, taking into account the dynamic processes in the driving system under the conditions of the variable adhesion of road wheels. The model of interaction between a tired wheel and the terrain takes into account the relationship between the road wheel adhesion factor and the slipping action, as well as the impacts of the differential gear on distribution of drive torque. The 3D (spatial) model of a backhoe loader is considered. It is a two-axle self-propelled machine on a wheeled chassis. The mathematical model constitutes nonlinear and non-stationary differential equations of motion. Their stability is therefore associated with vibration intensity. Simulations in the time domain were supported by Matlab-Simulink. The purpose of this study is to improve the safety features during the ride of mobile heavy machines, basing on the parametric optimization of the model.

Keywords: *spatial model, dynamic system, mobile heavy machines, unsprung vehicles, 'galloping' effect, snake meandering" effect, adhesion factor, slipping action, vibration, differential gear*

1. Physical model of an unsprung wheeled machine

In the context of potential possibility of the "snake meandering" effect during the ride of a mobile, wheeled machine, the spatial model of an excavator-loader (Fig. 1) is implicated for further considerations. The excavator-loader is an unsprung machine in which the frame is rigidly connected to the axles. The front axle can perform independent oscillations relative to the machine body, described by coordinate ψ_1. Two local coordinate systems are introduced, the one associated with the rocker has its origin – O_w on its axis of rotation, the other system is associated with the base of the machine, its origin coinciding with the centre of gravity of the machine – S_0. At that stage, the flexibility of fluid cells in the implements is neglected.

The motion of the machine is expressed in the coordinate system relative to the inertial frame, which, at the initial moment, coincides with a local system associated with the machine. Relationships between the systems are expressed by transformation matrices. Transformation matrices for rotation relative to the main axis of the system are given below [3]:

$$\mathbf{T}_X(\psi)=\begin{bmatrix}1 & 0 & 0\\ 0 & cos(\psi) & -sin(\psi)\\ 0 & sin(\psi) & cos(\psi)\end{bmatrix},\mathbf{T}_Y(\delta)=\begin{bmatrix}cos(\delta) & 0 & sin(\delta)\\ 0 & 1 & 0\\ -sin(\delta) & 0 & cos(\delta)\end{bmatrix},\mathbf{T}_Z(\varphi)=\begin{bmatrix}cos(\varphi) & -sin(\varphi) & 0\\ sin(\varphi) & cos(\varphi) & 0\\ 0 & 0 & 1\end{bmatrix}. \quad (1)$$

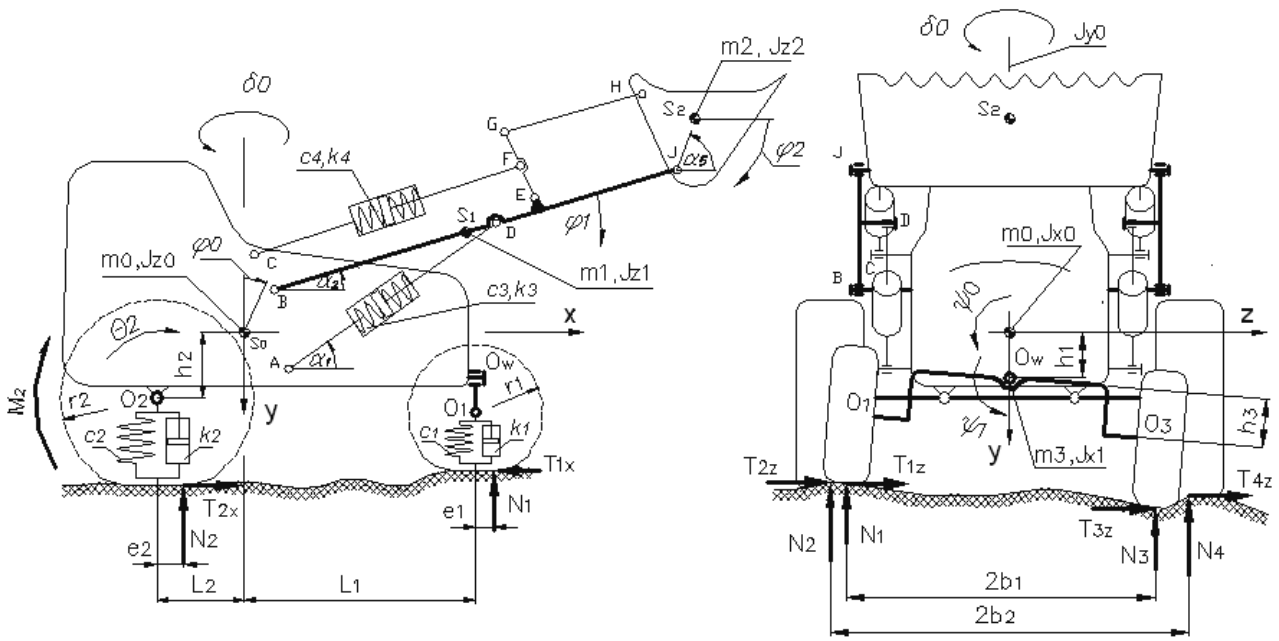

Fig. 1. Physical model of a two-axle wheeled machine

Respective coordinates of joint "O_w" and the coordinates of the wheel axis "O_i" with respect to the moving coordinates system associated with the body of the machine are obtained basing on Fig. 1:

$$\mathbf{O}_W = \begin{bmatrix} x_W \\ y_W \\ z_W \end{bmatrix} = \mathbf{T}_Z(\varphi)\cdot\mathbf{T}_y(\delta)\cdot\mathbf{T}_X(\psi)\cdot\begin{bmatrix} L_1 \\ h_1 \\ 0 \end{bmatrix}, \tag{2}$$

$$\mathbf{O}_1 = \begin{bmatrix} x_1 \\ y_1 \\ z_1 \end{bmatrix} = \mathbf{T}_Z(\varphi)\cdot\mathbf{T}_y(\delta)\cdot\mathbf{T}_X(\psi)\cdot\left[\mathbf{T}_X(\psi_1)\cdot\begin{bmatrix} 0 \\ h_3 \\ -b_1 \end{bmatrix} + \begin{bmatrix} L_1 \\ h_1 \\ 0 \end{bmatrix}\right], \tag{3}$$

$$\mathbf{O}_3 = \begin{bmatrix} x_3 \\ y_3 \\ z_3 \end{bmatrix} = \mathbf{T}_Z(\varphi)\cdot\mathbf{T}_y(\delta)\cdot\mathbf{T}_X(\psi)\cdot\left[\mathbf{T}_X(\psi_1)\cdot\begin{bmatrix} 0 \\ h_3 \\ b_1 \end{bmatrix} + \begin{bmatrix} L_1 \\ h_1 \\ 0 \end{bmatrix}\right], \tag{4}$$

$$\mathbf{O}_2 = \begin{bmatrix} x_2 \\ y_2 \\ z_2 \end{bmatrix} = \mathbf{T}_Z(\varphi)\cdot\mathbf{T}_y(\delta)\cdot\mathbf{T}_X(\psi)\cdot\begin{bmatrix} -L_2 \\ h_2 \\ -b_2 \end{bmatrix}, \tag{5}$$

$$\mathbf{O}_4 = \begin{bmatrix} x_4 \\ y_4 \\ z_4 \end{bmatrix} = \mathbf{T}_Z(\varphi)\cdot\mathbf{T}_y(\delta)\cdot\mathbf{T}_X(\psi)\cdot\begin{bmatrix} -L_2 \\ h_2 \\ b_2 \end{bmatrix}, \tag{6}$$

When $\mathbf{J}_i$, $\mathbf{J}_j$ are Jacobian matrices, and $\mathbf{V}_0 = [V_{0x}\ V_{0y}\ V_{0z}]^T$ – is the velocity vector of the centre of gravity of the machine – S_0, the velocity vectors of front and rear wheels respectively are given by (8) and (10):

$$\mathbf{J}_i = \begin{bmatrix} \frac{\partial x_i}{\partial \psi_1} & \frac{\partial x_i}{\partial \psi_0} & \frac{\partial x_i}{\partial \delta_0} & \frac{\partial x_i}{\partial \varphi_0} \\ \frac{\partial y_i}{\partial \psi_1} & \frac{\partial y_i}{\partial \psi_0} & \frac{\partial y_i}{\partial \delta_0} & \frac{\partial y_i}{\partial \varphi_0} \\ \frac{\partial z_i}{\partial \psi_1} & \frac{\partial z_i}{\partial \psi_0} & \frac{\partial z_i}{\partial \delta_0} & \frac{\partial z_i}{\partial \varphi_0} \end{bmatrix}, \ where: i = 1,\ 3. \tag{7}$$

$$\mathbf{V}_i = \mathbf{V}_0 + \mathbf{J}_i \begin{bmatrix} \omega_{x1} & \omega_x & \omega_y & \omega_z \end{bmatrix}^{\mathrm{T}}, \ where: i = 1,\ 3. \tag{8}$$

$$\mathbf{J}_j = \begin{bmatrix} \frac{\partial x_j}{\partial \psi_0} & \frac{\partial x_j}{\partial \delta_0} & \frac{\partial x_j}{\partial \varphi_0} \\ \frac{\partial y_j}{\partial \psi_0} & \frac{\partial y_j}{\partial \delta_0} & \frac{\partial y_j}{\partial \varphi_0} \\ \frac{\partial z_j}{\partial \psi_0} & \frac{\partial z_j}{\partial \delta_0} & \frac{\partial z_{ji}}{\partial \varphi_0} \end{bmatrix}, \ where: \ j = 2,\ 4. \tag{9}$$

$$\mathbf{V}_j = \mathbf{V}_0 + \mathbf{J}_j \begin{bmatrix} \omega_x & \omega_y & \omega_z \end{bmatrix}^{\mathrm{T}}, \ where: \ j = 2,\ 4. \tag{10}$$

Indices i and j correspond to wheel designations in Fig. 1.

2. Model of the drive system including the differential

The dynamics of the machine movement is determined by the properties of its drive system, such as torque-velocity characteristic of the engine and power transmission to the wheels in the differential. A conventional propulsion system is considered, equipped with a mechanical (manual) gearbox, its schematic diagram is not provided here, as it is a widely known solution. The model of a differential is shown in Fig. 2.

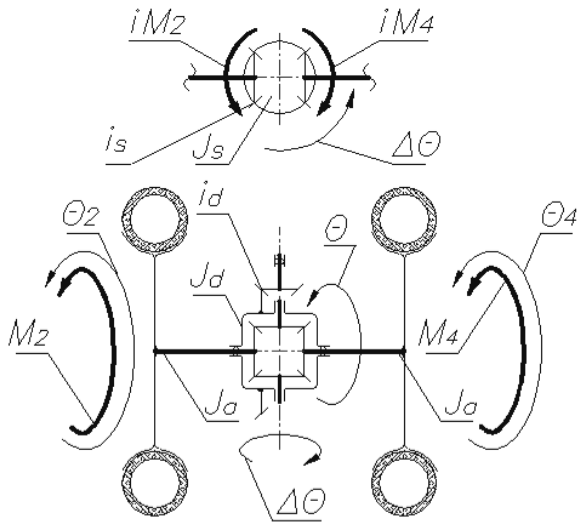

Fig. 2. Differential model

The mass moment of inertia of the drive system J_θ reduced to the crown wheel is expressed by the relationship:

$$J_\theta = m_C \cdot r_C^2 + \beta \cdot J_a, \tag{11}$$

where:
m_c – total mass of the machine,
r_{2s} – static radius of the driving wheel,
J_a – mass moment of inertia of a wheel with the driveshaft,
β – moment of inertia (normalized with respect to J_a) of the whole kinematic chain formed by a crank mechanism engine, clutch, shafts and gears depending to the current gear ratio gearing, main basket satellites and both wheels with axle shafts.

Torque to the drive wheels is effected by the differential whose mass moment of inertia $J_{\Delta\theta}$ is given as (12):

$$J_{\Delta\theta} = 2 \cdot J_a \cdot i_s. \tag{12}$$

Inertia of satellites – J_s is omitted as negligible compared to J_a, transmission ratio $i_s = 1$.

The angular velocity of the driving wheel is dependent on the motor loading. The torque vs angular velocity characteristic of a diesel engine 3054C Caterpillar, reduced to the crown wheel, is shown in Fig. 3. The plot graphed with heavy line $\alpha = 1$ represents the maximal torque developed for the full dose of fuel. For smaller loads, the desired ride velocity is reached with a smaller dose of fuel supplied by the feed pump designated as α = 0.9, α = 0.7, α = 0.6, are graphed with fine lines [2].

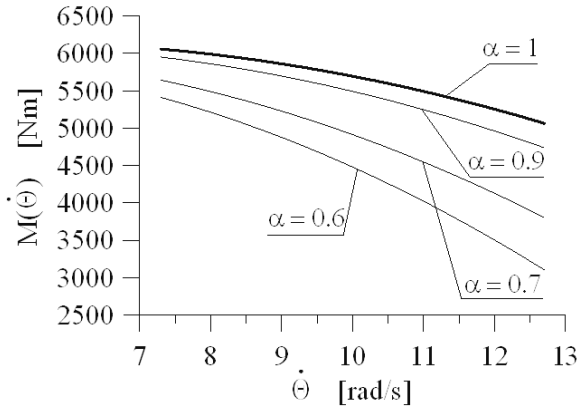

Fig. 3. Torque vs angular velocity of an engine reduced to the to the crown wheel, for variable fuel doses

3. The model of cooperation wheels with the ground

Ride over uneven ground is accompanied by dynamic variable reactions acting on the wheel. The vertical response of the roadway surface to loads – N_i, exerted by wheels is shifted in relation to the geometric axis of the wheel rotation [2, 6].

The magnitude of this eccentricity – e_i is a variable quantity as it is related to the dynamic wheel radius – r_{iD} through a dimensionless resistance factor f_i:

$$f_i = \frac{e_i}{r_{iD}}, \quad \text{where: } i = 1,3. \tag{13}$$

The value of the rolling resistance of a tired wheel depends on the roadway surface and ride velocity. In a narrow range of velocities, the rolling resistance is taken to be constant, dependent solely on the roadway surface conditions.

The notation of damping forces acting in the radial and circumferential directions takes into account the dependence between the damping factor in the tire and vibration frequency – ω [5]:

$$k_i = c_i \frac{\delta}{\omega}, \text{where: } i = 1, 2, 3, 4, \tag{14}$$

where:
δ – coefficient of energy dissipation related to the type of tires, typically $\delta \in [0.1\text{-}0.2]$,
c_i – stiffness of wheel tires of a given axle in the radial direction.

Dynamic reactions acting on the wheel sideways were determined using the Dugoff's model [7, 8]. They are related to the pressure values of N_i, and are the result of the combined elastic deformation and friction of the tire. The motion of tired wheels will always involve certain slipping. Longitudinal forces can be expressed as the product of [1, 2, 4, 6]:

$$T_{ix} = \mu_{ix}(S_{ix})N_i, \text{where}: i = 2, 4. \tag{15}$$

The longitudinal slip rate – S_{ix} expresses the relative difference between linear velocities of the axles in the horizontal direction resulting from the rotating motion (no slippage) and the real velocity [1, 5]. In the case when $d\theta_i/dt > 0$:

$$S_{ix} = 1 - \frac{V_{ix}}{r_{iD} \cdot \theta_i}, \quad \text{where: } i = 2, 4. \tag{16}$$

The relationship between the coefficient of longitudinal road adhesion and the slip rate for various roadway conditions is modelled by a bi-parametric function $o_x(S_x)$ [2].
This function can be determined as long as the maximal coefficient of road adhesion – μ_{max} (reached under the critical slippage conditions – S_{xkr}.) can be found for the given roadway surface.

$$\mu(S_{ix}) = \frac{\mu_1 \cdot S_{ix}}{\left(\mu_2 + |S_{ix}|\right)^2}, \tag{17}$$

$$\mu_{max} = \mu(S_{xkr}) \Rightarrow \begin{cases} \mu_1 = \mu_{max} 4S_{xi}, \\ \mu_2 = S_{xkr}. \end{cases} \tag{18}$$

The function $o_x(S_x)$ expressed by (5) and (6) is a simplified version of the best known descriptions of the tire – road surface impacts: the Magic Formula of Pacejka [1, 7], the Dugoff Tire Model [1, 7], the LuGre model [8]. Selected plots of the function $o_x(S_x)$ for diverse road conditions are shown in Fig 4. The lateral slip rate – S_{iz} depends on the longitudinal slip and the slip angle – a_i of ith wheel [1, 7, 8]:

$$S_{iz} = (1 - S_{xi})tg(\alpha_i) = -(1 - S_{xi})\frac{V_{iz}}{V_{ix}}, \text{ where: } i = 2, 4. \tag{19}$$

Lateral reactions can be expressed in an analogous relationship to (15):

$$T_{iz} = \mu_{iz}(S_{iz})N_i, \text{ where: } i = 2, 4. \tag{20}$$

The relationship between the coefficient of lateral road adhesion and the slip rate – $\mu_{iz}(S_{iz})$ for various roadway conditions is taken from [1, 4, 6].

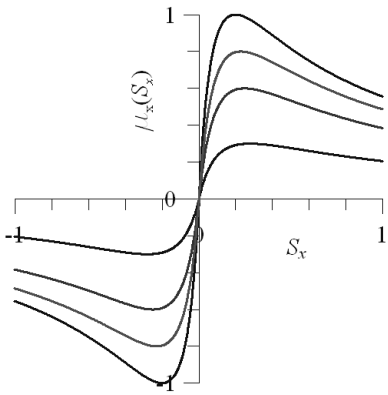

Fig. 4. Coefficient of road adhesion in longitudinal direction vs. slip rate for various roadway surfaces

4. Vibrations of an unsprung wheeled machine

The equations of motion of the vehicle shown in Fig. 1 during the ride, taking into account the distribution of the torque to the right and left drive wheel via the differential depending on the actual adhesion conditions are given below:

$$\mathbf{M}\cdot\frac{d}{dt}\begin{bmatrix}\dot{x}_0\\ \dot{y}_0\\ \dot{z}_0\\ \dot{\varphi}_0\\ \dot{\varphi}_1\\ \dot{\delta}_0\\ \dot{\psi}_0\\ \dot{\theta}\\ \Delta\dot{\theta}\end{bmatrix}=\begin{bmatrix}T_{2x}+T_{4x}-f_1N_1-f_3N_3\\ m_Cg-N_1-N_2-N_3-N_4\\ T_{1z}+T_{2z}+T_{3z}+T_{4z}\\ y_w(T_{1z}+T_{3z})+z_w(N_1+N_3)+y_2T_{2z}+y_4T_{4z}+z_2N_2+z_4N_4\\ (y_1-y_w)T_{1z}+(y_3-y_w)T_{3z}+(z_1-z_w)N_1+(z_3-z_w)N_3\\ (-1)x_w(T_{1z}+T_{3z})-z_w(T_{1x}+T_{3x})-x_2T_{2z}-x_4T_{4z}+z_2T_{2x}+z_4T_{4x}\\ (-1)x_w(N_1+N_3)+y_w(T_{1x}+T_{3x})-x_2N_2-x_4N_4-y_2T_{2x}-y_4T_{4x}\\ M(\dot{\theta})-M_2(\dot{\theta}-\Delta\dot{\theta})-M_4(\dot{\theta}+\Delta\dot{\theta})\\ M_2(\dot{\theta}-\Delta\dot{\theta})-M_4(\dot{\theta}+\Delta\dot{\theta})\end{bmatrix}, \tag{21}$$

where:

$\mathbf{M}=diag\lfloor m_C \quad m_C \quad m_C \quad J_{x0} \quad J_{x1} \quad J_{y0} \quad J_{z0} \quad J_\theta \quad J_{\Delta\theta}\rfloor$ – matrix of inertia,

J_{x0}, J_{y0}, J_{z0} – total inertia moments of the machine with respect to the main axes of the machine,

J_{x1} – mass moment of inertia with respect to the rocker pin,

$\dot{\theta}$ – the angular velocity of the crown wheel,

$M(\dot{\theta})$ – torque reduced to the crown wheel,

$M_{2(4)}(\dot{\theta}\mp\Delta\dot{\theta})$ – resisting torques on the drive shafts.

Computer simulations, supported by Matlab-Simulink and Mathcad, were performed for the applied kinematic excitations. The angular velocity of the driving wheel in the steady state – θ_s was taken to be 10 rad/s. Parameters of the machine configured as in Fig. 1 are: $m_C = 9420$ [kg], $J_{x0} = 2273$ [kgm^2], $J_{x1} = 12.3$ [kgm^2], $J_{y0} = 3370$ [kgm^2], $J_{z0} = 10427$ [kgm^2], $L_1 = 0.9509$ [m], $L_2 = 1.1491$ [m], $h_1 = 0.5095$ [m], $h_2 = 0.3095$ [m], $r_{s1} = 0.4335$ [m], $r_{s2} = 0.6701$ [m], $c_1 = 7.676 \cdot 10^5$ [N/m], $c_2 = 1.383 \cdot 10^6$ [N/m], $f_1 = f_2 = 0.03$ [-], $\delta = 0.2$ [-].

The tire stiffness in the radial direction and then in longitudinal direction was obtained by applying procedures outlined in [1, 4].The characteristics obtained for simulations of a ride with a full load bucket – 2000 [kg] are graphed with heavy thick line, with fine lines – for the ride with no excavated material. At this stage, the main focus is on simulating the effect of the tear-off front and rear wheels. Dynamic pressure normalization was done with respect to the static values.

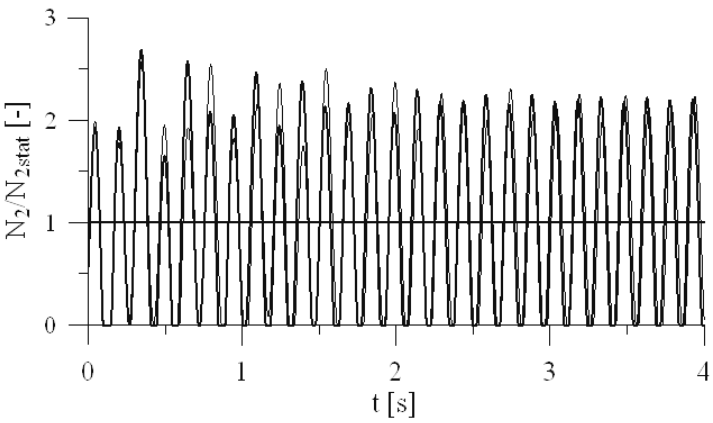

Fig. 5. Normalized dynamic pressure of the rear wheels in the function of time

Figure 5 reveals a strong tendency to tear the wheels of the rear axle from the ground at speeds below 24 km /h. The presence of bucket load practically does not change this trend.

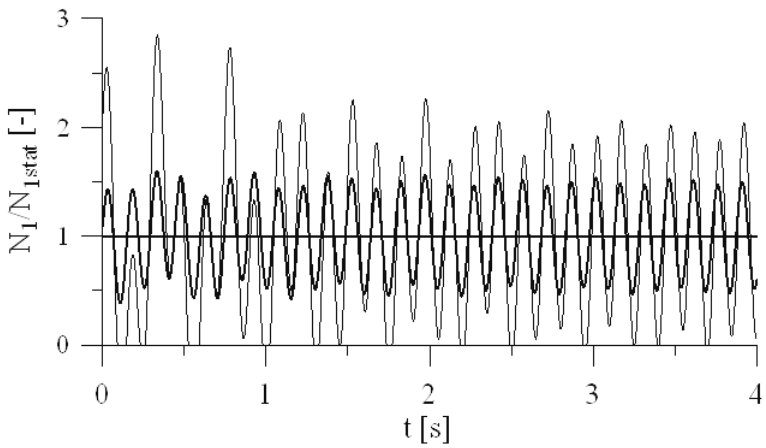

Fig. 6 Normalized dynamic pressure of the front wheels in the function of time

As shown in Fig. 6, ride without loading the bucket introduces the risk of a loss of steering when the road wheels break away from the road surface. Driving with excavated material improves the steering behaviour of the machine by increasing the pressure of the front axle.

Since the dynamic component of pressure acting upon the axle wheels during the ride with and without bucket load exceed the static component – the ride becomes irregular power and the forward motion becomes "jerky," as shown in Fig. 7. Because of the energy loss due to friction between wheels and uneven surfaces, the vehicle moves forward at an average rate of a few percent lower than if the ride took place in the same environment and loading conditions, but over a smooth surface. Characteristic inflection points corresponds to the moments when the rear wheels of break away from the road surface, in the conditions where $N_{2(4)} = 0$.

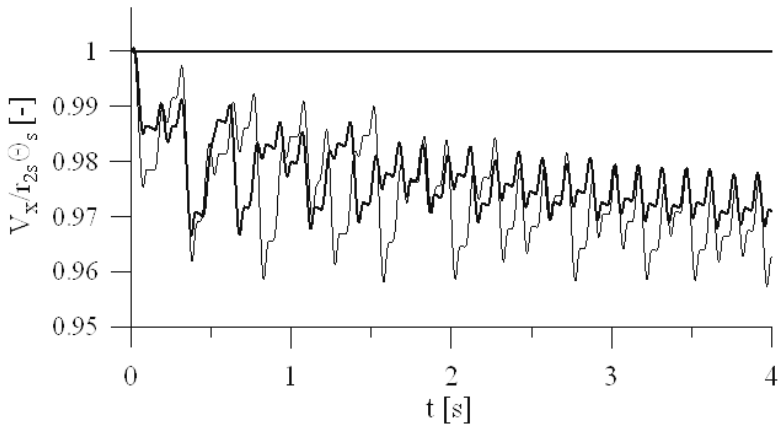

Fig. 7. Changing the driving speed with and without load bucket normalized to the speed of movement on the smooth surface

Flexibility of wheel tires significantly reduces the dynamic loading of the driving system.

Kinematical interactions of tires with the roadway surface are implemented in the conditions of variable road adhesion and slip rate. During one cycle of vibration, both the coefficient of road adhesion and the slip rate change both their magnitude and sign.

5. Conclusion

The spatial model of unsprung wheeled machine considered in this study allows the analysis of safety and comfort features during the ride, proving the susceptibility of unsprung machines on

wheeled chassis to “galloping.” Its full potential as a spatial model will be used in research on “snake meandering” effect" and motion stability while driving around a curve.

Simulation results shown in Fig. 5-7 agree well with observations of the behaviour of machines on the road. Undoubtedly, there is a need for road tests for verification of the simulation model so that the model should be used as a tool in parametric optimization.

References

[1] Andrzejewski, R., Awrejcewicz, J., *Nonlinear Dynamics of a Wheeled Vehicle*, Springer Science+Business Media, Inc., 2005.

[2] Chwastek, S., *Modal stability control of a wheeled heavy machine*, Applied Mechanics and Materials, Vol. 477-479, pp. 69-72, doi:10.4028, 2014.

[3] Craig, J., *Introduction to robotics: mechanics and control*, Addison-Wesley Publishing Inc., Massachusetts USA 1989.

[4] Grzegożek, W., *Modelowanie dynamiki samochodu przy stabilizującym sterowaniu siłami hamowania,* Monografia 275, Wydawnictwo Politechniki Krakowskiej, Kraków 2000.

[5] Mitschke, M., Wallentowitz, H., *Dynamik der Kraftfahrzeuge*, Springer, 2004.

[6] Prochowski, L., *Mechanika ruchu. Pojazdy samochodowe*, WKŁ, Warszawa 2005.

[7] Sorniotti, A., Vigiliani, A, *Numerical models for tyres simulation*, AITC-AIT 2006, International Conference on Tribology, Parma, Italy 2006.

[8] Tsiotras, P., Velenis, E., Sorine, M., LuGre, A, *Tire Friction Model with Exact Aggregate Dynamics*, Proceeding of the American Control Conference Boston, Massachusetts 2004.